Hydrometallurgy 102 (2010) 43–49

Contents lists available at ScienceDirect

Hydrometallurgy

journal homepage: www.elsevier.com/locate/hydromet

The kinetics of zinc silicate leaching in sodium hydroxide

Fabiano M.F. Santos, Pablo S. Pina, Rodrigo Porcaro, Victor A. Oliveira, Carlos A. Silva, Versiane A. Leão *

Bio and Hydrometallurgy Laboratory — Department of Metallurgical and Materials Engineering, Universidade Federal de Ouro Preto, Campus Morro do Cruzeiro, s.n. 35400-000, Ouro Preto, MG, Brazil

ARTICLE INFO

Article history:
Received 6 September 2009
Received in revised form 16 December 2009
Accepted 30 January 2010
Available online 6 February 2010

Keywords:
Zinc silicate
Sodium hydroxide
Leaching kinetics
Shrinking particle model
Chemical control

ABSTRACT

The alkaline leaching kinetics of a zinc silicate ore assaying 34.1% Zn, 11.1% Fe and 22.9% SiO_2 is studied in sodium hydroxide solutions. Speciation diagrams indicate zinc dissolution as $[Zn(OH)_4]^{2-}$ and SEM analysis showed a progressive reduction in particle size during leaching which supports the shrinking particle model. The process is chemically controlled with an activation energy of 67.8 ± 9.0 kJ/mol and reaction order with respect to NaOH determined as 1.44 ± 0.46.

1. Introduction

Zinc is mainly produced by the roasting–leaching–electrolysis route (RLE) which combines pyro- and hydrometallurgical operations. However, with the development of the acid leaching (AL)–solvent extraction (SX)–electrowinning (EW) process, non-sulphide zinc deposits now account for about 10% of world metallic zinc production. Unlike zinc sulphides treated by the RLE route, the processing of zinc silicates can follow different approaches. Solvent extraction is one alternative, while some companies have integrated zinc silicate and zinc sulphide leaching (Souza, 2007). Both routes use acid leaching to dissolve zinc from the ores/concentrates and special care is taken to avoid the formation of silica gel. This can be achieved by a stepwise addition of sulphuric acid, whereby the silicate is dissolved with a minimum silica gel formation (Souza et al., 2009).

The acid leaching of oxidized zinc ores and concentrates has some drawbacks. This is because zinc carbonates (smithsonite, $ZnCO_3$; hydro-zincite, $2ZnCO_3 \cdot 3Zn(OH)_2$) and silicates are generally acid consumers. Also, they are usually associated with other acid consuming gangue minerals such as calcium carbonate. Therefore, for an efficient acid leaching of such materials, the content of the gangue minerals needs to be reduced which is usually attained by a concentration step. This sometimes results in large volumes of carbonate containing tailings with fairly reasonable zinc content for which a cost-effective leaching route is yet to be developed.

Zinc leaching from carbonate and oxide ores can be addressed applying alkaline solutions. Frenay (1985) studied the leaching of oxidized zinc ores in various solution media and pointed out the best results with caustic soda. The leaching in alkaline media (ammonia, caustic soda, and diethylene-triammine) showed that hemi-morphite could be leached with caustic soda at high temperature (85 °C). Ammonium carbonate enhanced the leaching of hemi-morphite but decreased that of smithsonite. Zhao and Stanforth (2000) studied the production of zinc powder by an alkaline treatment of smithsonite ores and observed that over 85% zinc could be leached at 90–95 °C, in 1.5 h with 5 mol/L NaOH. The alkaline leaching of a low grade smithsonite ore was also carried out in columns after pelletizing the ore with cement. The best results showed over 80% zinc dissolution for a 20 days leaching period (Feng et al., 2007).

The leaching kinetics of zinc ores and concentrates has been studied by many researchers (Bobeck and Su, 1985; Bodas, 1996; Feng et al., 2007; Ghosh et al., 2002), especially in sulphuric acid solutions (Abdel-Aal, 2000; Terry and Monhemius, 1983). The shrinking core model, SCM, (Levenspiel (1962)) was applied to describe the leaching data in most of those studies. Bodas (1996) studied the leaching kinetics of two different zinc ores and noticed that the leaching kinetics was diffusion-controlled with activation energies varying from 4 to 17 kJ/mol. Maximum zinc extractions reached 95% at 70 °C and 4.5 mol/L H_2SO_4, in 3 h. Terry and Monhemius (1983) have comprehensively studied the leaching kinetics of natural hemi-morphite, as well as natural and synthetic willemite. The authors observed that the acidic dissolution was diffusion-controlled for hemi-morphite and chemically-controlled for willemite leaching. Abdel-Aal (2000), studying the leaching kinetics of low grade zinc silicate, proposed that the process was

* Corresponding author. Tel.: +55 31 3559 1102; fax: +55 31 3559 1561.
E-mail address: versiane@demet.em.ufop.br (V.A. Leão).

0304-386X/$ – see front matter © 2010 Elsevier B.V. All rights reserved.
doi:10.1016/j.hydromet.2010.01.010

Table 1
Chemical analysis and surface area of zinc silicate concentrate screened fractions.

Parameter	Unit	Size fraction 105–75 μm	Size fraction 75–53 μm	Size fraction 53–45 μm	Size fraction 45–38 μm
Zn	(%)	39.7	35.6	35.2	34.1
Fe	(%)	9.8	11.7	10.3	11.1
SiO_2	(%)	24.3	23.8	23.2	22.9
Surface area	m^2/g	1.0	0.6	0.6	1.0
Total porous vol.	mm^3/g	3.3	2.5	2.5	2.5
Pore ave. diameter	Nm	13.1	17.9	18.0	9.8

controlled by diffusion on an "ash" layer with an associated activation energy of 13.4 kJ/mol.

When the SCM model was unsuccessful in describing the leaching kinetics, the grain pore model, GPM, (Szekely et al., 1976) was applied (Souza et al., 2007; Souza et al., 2009). It has been shown that if the transport through the pores of the solid is the rate-determining step, the GPM model predicts an expression similar to the shrinking core model (SCM) with diffusion control (Georgiou and Papangelakis, 1998). This approach was applied by Souza et al. (2007) to the acid leaching of zinc silicates and an activation energy of 59.5 ± 2.9 kJ/mol was obtained for the dissolution kinetics of a calcined zinc silicate. The same model was applied afterwards to the leaching of non-calcined zinc silicates containing either high (8–11%) or low (3%) iron content (Souza et al., 2009). The authors suggested that the iron content did not affect the leaching kinetics of the silicate concentrate as the activation energy was statistically similar for both materials (78.2 ± 12.1 kJ/mol and 66.8 ± 9.2 kJ/mol, for the high- and low-iron silicate, respectively). As the leaching kinetics in alkaline medium is far less studied than in acid solutions, the purpose of the present work is to assess the leaching kinetics parameters of a zinc silicate ore in sodium hydroxide.

2. Materials and methods

The zinc silicate concentrate contains 34–39% Zn (Table 1). The XRD of the calcine (measured with a Shimadzu 600 diffractometer equipped with an iron tube and graphite monochromator) showed the presence of willemite (Zn_2SiO_4) as the main zinc-containing phase as well as franklinite ($ZnO \cdot Fe_2O_3$) and hematite (Fe_2O_3) as minor constituents (Fig. 1). Mineralogical analysis also showed the presence of quartz and dolomite in the gangue (Souza et al., 2009) and the willemite content was estimated to be above 80%. Prior to the leaching experiments, the concentrate was dry ground and wet sieved to yield a particle size distribution between 150 and 38 μm. Zinc, iron and silica content as well as surface area, total porous volume and pore average diameter of the different sieved fractions are also presented in Table 1.

The chemical leaching experiments were carried out batch-wise in a closed water-jacket plastic reactor with 750 mL total volume. Agitation was provided by a magnetic stirrer (600 min^{-1}) that enabled adequate dispersion of the mineral particles without evaporation loss of the solution. The solution volume was 500 mL and the solid concentration 1 g/L.

Leaching solutions were prepared using reagent grade chemicals (NaOH, Synth) and distilled water. Unless otherwise stated, the leaching experiments were carried out using 38–45 μm particle size in 6 mol/L NaOH at 80 °C, and stirred at 600 min^{-1}. At selected time intervals, a known amount (3 mL) of slurry was withdrawn and filtered.

The zinc extraction was determined by analyzing zinc concentration in solution (after dilution in HCl), by atomic absorption spectrometry (Perkin Elmer AAnalyst 100), and for every sample withdrawn from the reactor, the volume change was taken into account for the zinc extraction determinations. The effects of temperature (60–90 °C), sodium hydroxide concentration (4–10 mol/L) and particle size (38 μm–105 μm) on the leaching kinetics were assessed.

Surface area and pore volume were determined by nitrogen adsorption. Nitrogen isotherms were performed with a Nova 1000 High Speed Gas Sorption Analyzer (Quantachrome). Sample degassing was carried out at 80 °C, for 24 h to avoid decomposition. Nitrogen adsorption was performed at −196 °C. Data were collected from a relative pressure (p/p_0) of 0.05 to 0.98. A large sample (~4.0 g) was used and the Nova 1000 parameters (equilibration tolerance, time to remain in tolerance and maximum equilibration time) were set at 0.05, 360 and 720, respectively, to improve the accuracy of low surface area measurements with nitrogen adsorption.

The morphological features of the concentrate, leach residues and reaction products formed during alkaline leaching were studied by

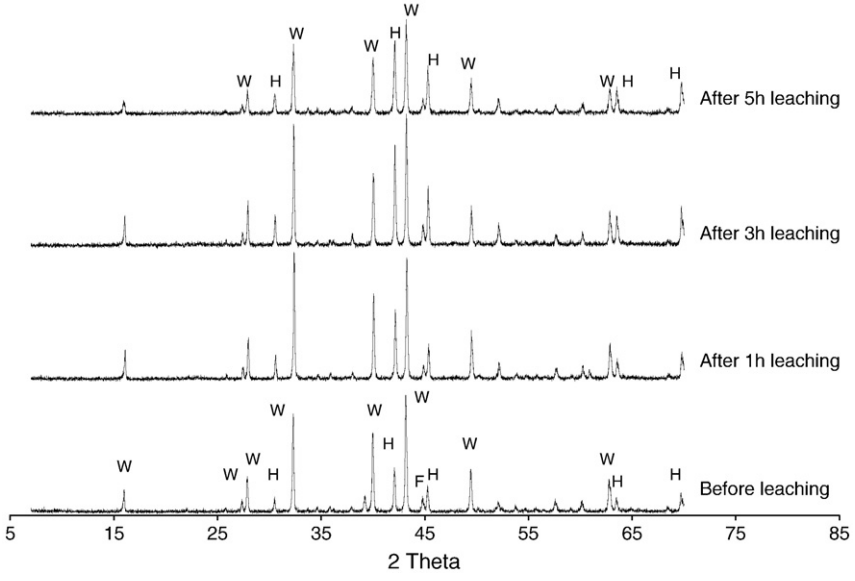

Fig. 1. XRD pattern of the zinc silicate concentrate. H: hematite, W: willemite, F: franklinite.

SEM–EDS. The particles investigated were filtered, carbon coated and then examined as a powder in a JEOL JSM 501 SEM microscope. Energy dispersive X-ray spectroscopy (EDS) was used for elemental analysis.

Statistical analysis was carried out using Origin™ version 8.0 software to determine the activation energy and reaction order with respect to NaOH for a 95% confidence interval.

3. Results and discussion

3.1. Outlining of the leaching system

The leaching of zinc compounds in sodium hydroxide solutions forms a series of hydroxy-complexes. Taking only the formation of mono-nuclear complexes, 4 different species can be found in the NIST database (Martell and Smith, 2003):

$$Zn^{2+} + OH^- \rightleftarrows [ZnOH]^+ \qquad \log\beta_1 = 5.0 \ (25\,^\circ C,\ I = 0) \qquad (1)$$

$$Zn^{2+} + 2OH^- \rightleftarrows [Zn(OH)_2]^0 \qquad \log\beta_2 = 11.1 \ (25\,^\circ C,\ I = 0) \qquad (2)$$

$$Zn^{2+} + 3OH^- \rightleftarrows [Zn(OH)_3]^- \qquad \log\beta_3 = 13.6 \ (25\,^\circ C,\ I = 0) \qquad (3)$$

$$Zn^{2+} + 4OH^- \rightleftarrows [Zn(OH)_4]^{2-} \qquad \log\beta_4 = 14.8 \ (25\,^\circ C,\ I = 0) \qquad (4)$$

Given the solid:liquid ratio applied during the experiments, the highest total zinc concentration is about 5.0×10^{-3} mol/L and therefore, for the experiments carried out with 6 mol/L NaOH, the free hydroxide concentration can be taken as equal to the nominal (initial) NaOH concentration. Fig. 2(a) depicts the molar fraction of the complexes presented in Eqs. (1)–(4), for the range of free OH^-concentration (mol/L) studied in the present work. As the figure shows, the predominance of $[Zn(OH)_4]^{2-}$is expected in the leaching system and accounts for >95% of the zinc species. Although the NIST Database does not present stability constants for higher temperatures and ionic strengths, the

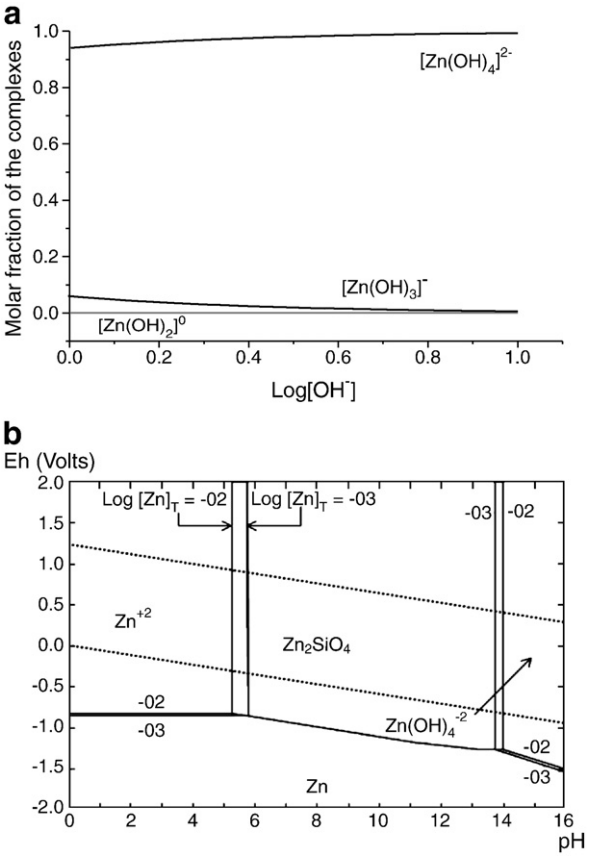

Fig. 2. (a) Speciation diagram of zinc hydroxy-complexes formed in alkaline systems. (b) Eh–pH diagram for willemite at 10^{-3} mol/L Si and different zinc concentrations. Temperature 25 °C, infinite dilution ($I = 0$). The species Zn^{2+}, $[ZnOH]^+$ and $[Zn(OH)_2]^0$ do not appear in the speciation diagram because their overall concentration is smaller than 1% of the total zinc species on the system.

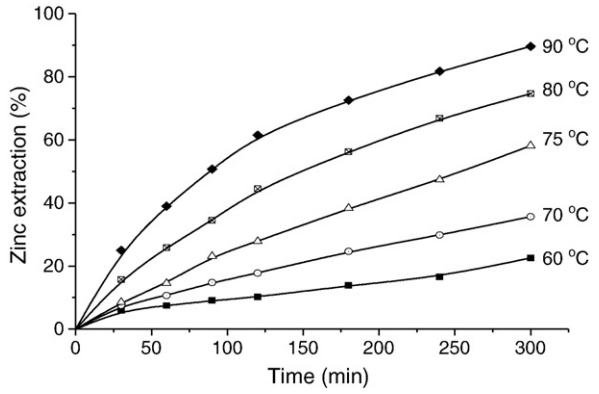

Fig. 3. Effect of temperature on zinc extraction with 6 mol/L NaOH. (1 g/L solids, stirring rate: 600 min^{-1}; particle size 45–38 μm).

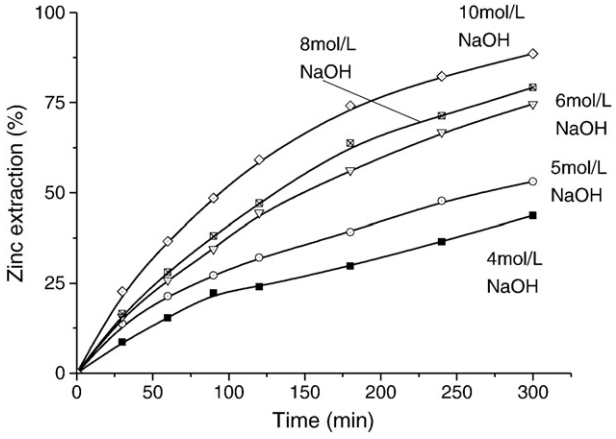

Fig. 4. Effect of NaOH concentration on zinc silicate extraction. (Temperature 80 °C; 1 g/L solids; 600 min^{-1}; particle size 45–38 μm).

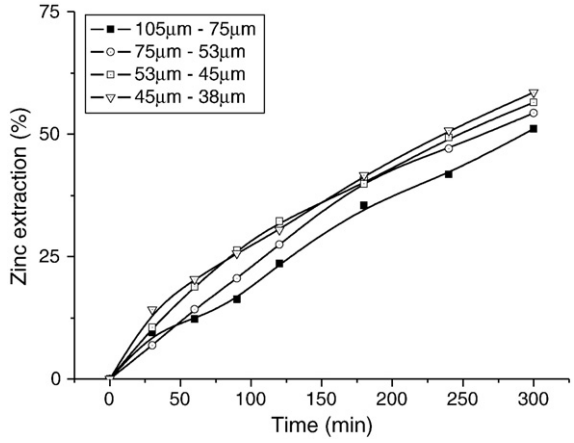

Fig. 5. Effect of particle size on zinc extraction. (80 °C; 1 g/L solids; 600 min^{-1}; 6 mol/L NaOH).

predominance of the $[Zn(OH)_4]^{2-}$ can be expected in the experimental conditions of the present work.

The formation of $[Zn(OH)_4]^{2-}$ in alkaline conditions can be also observed in the Eh–pH diagram depicted in Fig. 2(b). As expected, it also shows that willemite can be leached in acid solutions and the larger Zn^{2+} stability region provides easier dissolution at low pH conditions. However, according to Frenay (1985) the nature of the ore, especially the gangue minerals, will define the acid or alkaline leaching route. As NaOH does not react extensively with carbonaceous materials, it could be applied to both oxidized zinc ores and residues where there is a high content of carbonaceous minerals. Nevertheless, to ensure high zinc dissolution, NaOH concentrations should be high and the solution viscosity may play an important role on the leaching process.

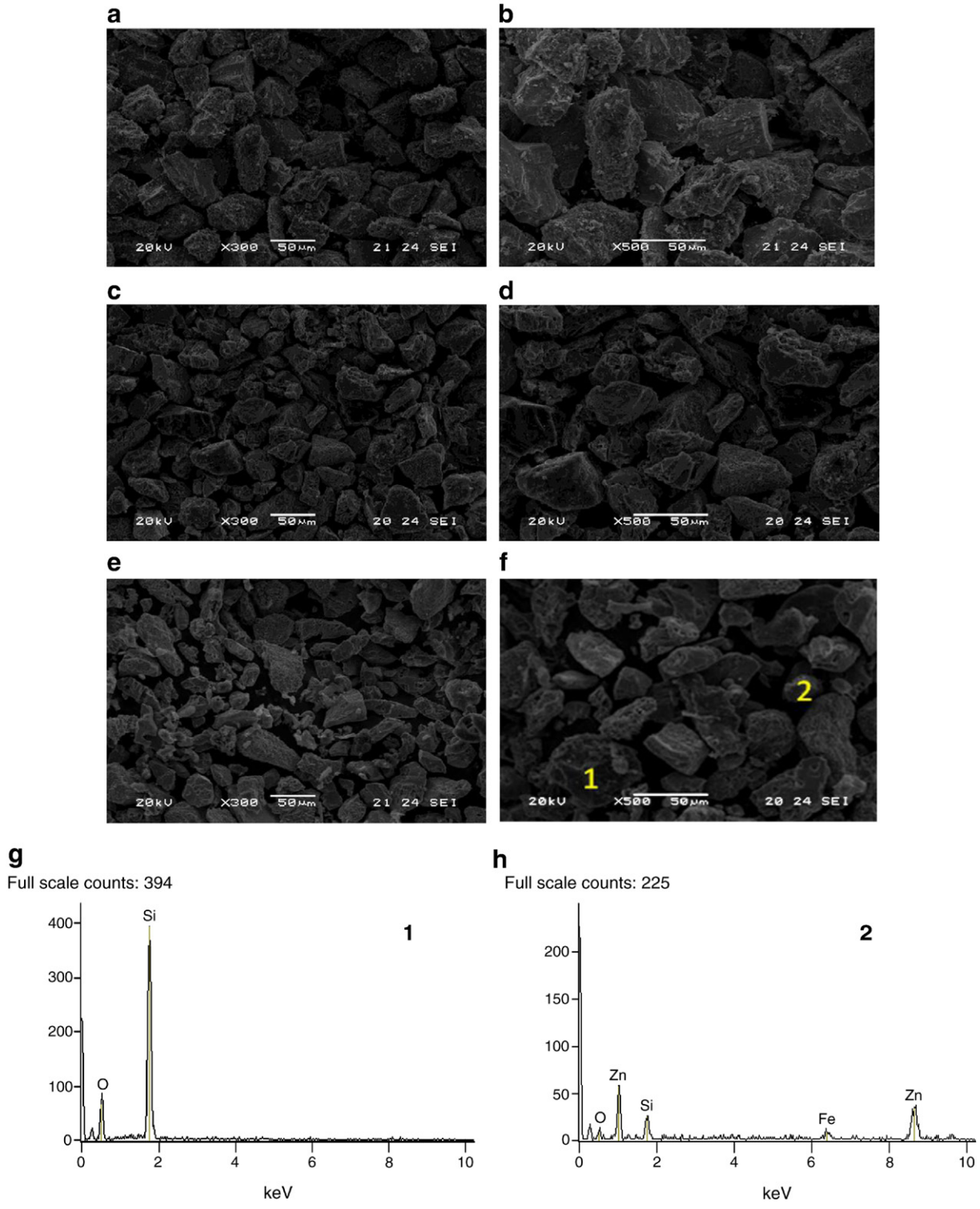

Fig. 6. (a, b) Particles of zinc silicate ore before leaching; (c, d) after 3 h leaching; and (e, f) after 5 h leaching. Figures (a, c, e) ×300; Figures (b, d, f) ×500. Figures (g) and (h) EDS spectra of particles 1 and 2 in Figure f. (Leaching conditions: 10 mol/L NaOH, 80 °C, 600 min^{-1}, 2 g/L solids).

Following Fig. 2, zinc is leached in sodium hydroxide as $[Zn(OH)_4]^{2-}$ and according Habashi (1993), Zaky et al. (2008) and Chen et al. (2009), a likely representation of willemite dissolution is:

$$2ZnO.SiO_{2(s)} + 6OH^-_{(aq)} + H_2O \rightarrow 2[Zn(OH)_4]^{2-} + SiO_3^{2-}(aq) \quad (5)$$

3.2. Effects of temperature, particle size and NaOH concentration on zinc extraction

Fig. 3 presents the effect of temperature on the dissolution of the zinc silicate ore in the 60 °C–90 °C range. The results indicate that 5 h are required for the complete leaching of the ore and that zinc extraction can reach 90% at the highest temperature tested. The temperature strongly influences the zinc dissolution as an increase of 20 °C in this variable (from 70 °C to 90 °C) enhances the dissolution from 36% to 90%. These results are consistent with the work of Dutra et al. (2006) who studied the leaching of electric arc furnace (EAF) dusts. The authors observed 74% zinc dissolution with 6 mol/L NaOH, in 4 h. Similar conclusions were also obtained by Bodas (1996) and Espiari et al. (2006), who carried out leaching experiments with a zinc silicate ore containing hemi-morphite ($Zn_4Si_2O_7(OH)_2 \cdot H_2O$) and smithsonite ($ZnCO_3$) as major zinc minerals. Abdel-Aal (2000) also studied the leaching of a zinc silicate ore containing willemite and hemi-morphite as major zinc phases and observed that increasing the temperature from 40 °C to 70 °C improved zinc extraction from 70% to 95%. Similarly, Souza et al. (2009) verified that temperature influences the acid leaching of a zinc silicate calcine in the range of 30–60 °C, but to a lesser extent.

The effect of sodium hydroxide concentration on zinc extraction is depicted in Fig. 4. The results show that its concentration is important for zinc dissolution since zinc extraction improves from 50% to 90% when the NaOH concentration increases from 5 mol/L to 10 mol/L, Similarly, Jarupisitthorn et al. (2003) observed a positive effect on zinc dissolution from EAF dusts as a result of increasing the NaOH concentration to an optimum concentration of 2.5 mol/L. The authors attributed lower zinc extractions with 3 and 4 mol/L NaOH. to an increase in the solution viscosity. These results are in agreement with the work of Xia and Picklesi (2000) who noted an increase in zinc extraction from EAF dust from 0.7% to 11% as the NaOH concentration increased from 4 to 12 mol/L. In addition, an increase in solution viscosity was also observed which affected the solid–liquid separation step.

Fig. 5 presents the effect of particle size on zinc extraction and shows a decrease in particle size enhances zinc dissolution. However, particle size plays only a minor role in the leaching process. The zinc extraction achieved with particle sizes between 38 and 45 μm was only about 10% higher than that achieved with particle sizes in the range of 210–150 μm. This small difference is likely due to the negligible variation in both solid surface area (BET surface area) and porosity with particle sizes (Table 1). Massaci et al. (1998) similarly verified the non-significance of particle size in a factorial experiments carried out with a zinc sulphide ore in ferric sulphate media.

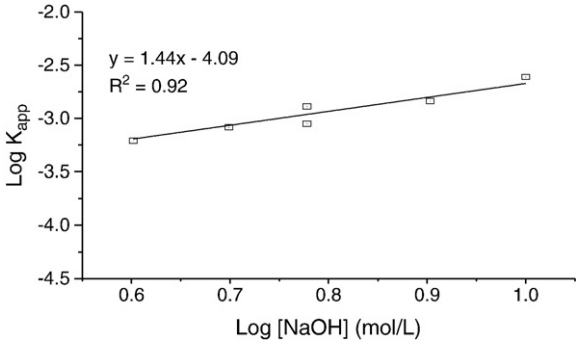

Fig. 8. Determination of reaction order with respect to NaOH concentration. (80 °C, 1 g/L solids, 600 min^{-1}; particle size: 45–38 μm).

3.3. Characterization of the leaching residues

The morphology of the zinc silicate concentrate before and during leaching was examined by SEM–EDS and is presented in Fig. 6. The solid particles before leaching show a narrow size distribution (Fig. 6a) as well as a natural rough surface (Fig. 6b). The micrographs of the leaching residues show a progressive reduction in particle diameter (Fig. 6c and d) and then an increase in roughness and porosity of the solids. For instance, after 60% Zn extraction (Fig. 6c and d), the particles show some size reduction that continues along the progress of ore dissolution (Fig. 6e and f). X-Ray and EDS analysis shows that the zinc-containing phases progressively disappear (Fig. 6f and h) while the less soluble hematite mineral predominates at later stages of leaching, as indicated in Fig. 1. Non-reactive quartz grains are also observed in the leaching residue (Fig. 6f and g).

These results are consistent with the findings of Dutra et al. (2006) who studied the alkaline leaching of EAF dusts.

3.4. Kinetic analysis

An irreversible and heterogeneous reaction of zinc silicate ores in sodium hydroxide solutions was assumed, where willemite was selectively leached. As there is a reduction in both the mass of solid and the particle size during leaching (Fig. 6), the shrinking particle model (Levenspiel, 1962) was applied to describe the leaching kinetics. Due to its simplicity, the shrinking core model has been chosen to study

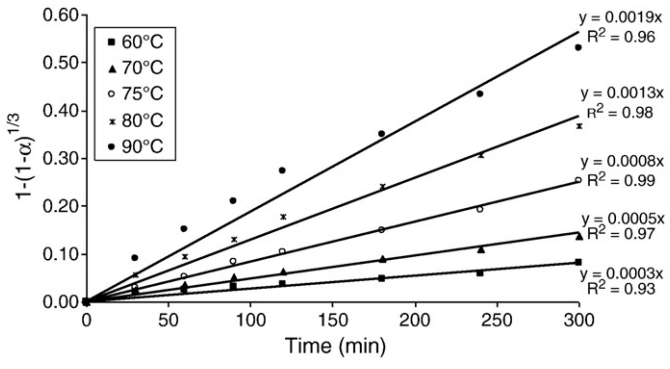

Fig. 7. Plot of shrinking core model for chemical reaction control. (6 mol/L NaOH, 1 g/L solids, 600 min^{-1}, particle size 45–38 μm).

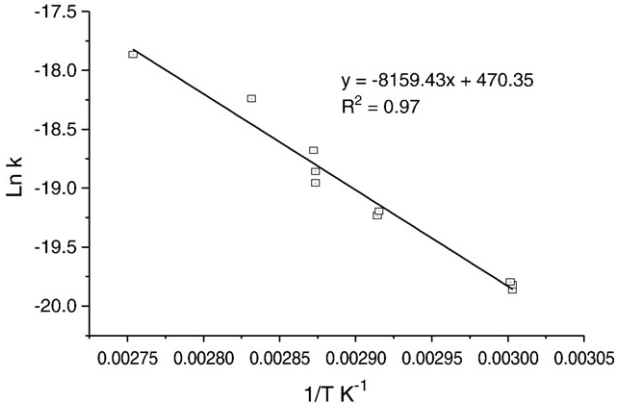

Fig. 9. Arrhenius plot of Ln rate constant versus $1/T$ for leaching zinc silicate. (6 mol/L NaOH, 1 g/L solids, 600 min^{-1}, particle size 45–38 μm).

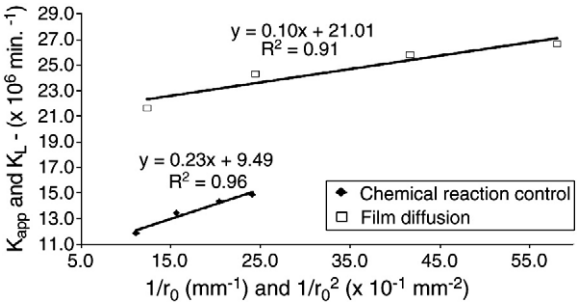

Fig. 10. Apparent rate constant versus inverse of particle size radius. (80 °C, 1 g/L solids, 600 min^{-1}, 6 mol/L NaOH).

heterogeneous leaching kinetics processes (Apostolidis and Distin, 1978; Boateng and Phillips, 1984; Senanayake, 2007) and specially zinc silicate leaching (Hursit et al., 2009; Teir et al., 2007).

If it is assumed that the zinc silicate particles have a spherical geometry and the chemical reaction is the rate-controlling step, then the following expression of the shrinking particle model can be used to represent the dissolution kinetics of the process:

$$1-(1-\alpha)^{1/3} = K_{app}.t, \quad \text{where } K_{app} = \frac{k.[NaOH]^n}{3.\rho_{solid}.R_o} \tag{6}$$

According to Eq. (6), a plot of $1-(1-\alpha)^{1/3}$ versus time is a straight line with slope K_{app} when the process is chemically controlled. As shown in Fig. 7, there is a good fit between the experimental data and Eq. (6), indicating that the leaching kinetics indeed can be described by the SCM model with chemical control.

Eq. (6) enables the reaction order to be determined with respect to NaOH. This was accomplished as the K_{app} can be written as $K_{app} = A.k.[NaOH]^n$. In this work, the reaction order with respect to NaOH was determined for a constant particle size (38–45 μm) and temperature (80 °C).

Fig. 8 shows the Log K_{app} versus Log [NaOH] plot from which the reaction order with respect to the NaOH concentration was determined as 1.44 ± 0.46. Both the value of reaction order and the stoichiometric coefficient of OH^- (i.e. 6 in Eq. (5)), imply that the alkaline leaching of willemite is a non-elementary process. As the process is chemically controlled, OH^- must adsorb and react at the particle surface producing two soluble compounds. This phenomenon is physically consistent with the hindering of silica gel formation and its further precipitation on the silicate surface. This process is similar to the silicate leaching control in acid medium (Safari et al., 2009).

The effect of temperature on the leaching kinetics can be characterized by the value of the activation energy. High values of activation energy (>40 kJ/mol) indicate chemical control whereas values <20 kJ/mol imply in diffusion-controlled processes (Levenspiel, 1962). Taking K_{app} as the angular coefficient in Eq. (6), the rate constant, k, can be determined from the values of reaction order (1.44), NaOH concentration (6000 mol/m^3), particle radius (41.10^{-6} m) and density (20795.1.mol/m^3). The rate constant is related to temperature according to the Arrhenius equation:

$$k = k_o \exp\left(-\frac{Ea}{RT}\right) \text{and} \, \text{Ln}(k) = \text{Ln}(k_o) - \frac{E_a}{R}.\frac{1}{T} \tag{7}$$

A plot of Ln k versus $1/T$ for the k values determined from Eq. (6), is a straight line where the slope is $(-E_a/R)$ (Fig. 9). Hence, the activation energy value was determined as 67.8 ± 9.0 kJ/mol chemical control appears to represent the mechanism of zinc silicate leaching kinetics with NaOH.

From the analysis of the shrinking core model with chemical reaction control (Eq. (6)) there appears to be a clear dependence of the model constant, K_{app} on the inverse of initial particle radius. Fig. 10 presents the plot of K_{app} versus $1/r_0$ and shows a linear relationship, further supporting the kinetic assumptions.

When the progressive dissolution of the silicate particles in sodium hydroxide is considered, another possible leaching mechanism is kinetic control by film diffusion (Levenspiel, 1962). When the largest resistance to the process is the diffusion through the boundary layer, the SCM predicts the following expression for the leaching kinetics of shrinking particles (Levenspiel, 1962):

$$1-(1-\alpha)^{2/3} = K_L.t \quad K_L = \frac{2.D.[NaOH]}{3.\rho_{solid}.R_o^2} \tag{8}$$

Notwithstanding, although a good fit was observed between K_L and $(1/R_o)^2$ (Fig. 9) and an activation energy of 69.8 ± 7.4 kJ/mol was determined from the diffusion coefficient achieved at different temperatures, the process is not film diffusion-controlled.

As already stated, the alkaline leaching kinetics of zinc-containing materials is far less studied than acid leaching kinetics and activation energy values vary considerably as shown in Table 2. An activation energy of 45.1 kJ/mol was determined for the sodium hydroxide leaching of EAF dusts by Jarupisitthorn et al. (2003), which is smaller than the value observed in this work. Nevertheless, both values are within the range of activation energies found in either acid or alkaline leaching of zinc ores (Table 2). Feng et al. (2007) proposed an ash

Table 2
Selected values of activation energies reported for the leaching of zinc silicates.

Experimental conditions	Model-controlling step	Activation energy (kJ/mol)	Reference
Hemi-morphite and willemite (26% ZnO/24% SiO_2), 5% solids. Leaching agent: H_2SO_4	Shrinking core model (SCM) — diffusion through product layer	13.4	(Abdel-Aal, 2000)
Smithsonite, hemi-morphite (37% ZnO/23.7% SiO_2); 2 mol/L H_2SO_4; 20–60 °C; particle size +53–75 μm; 5% solids	SCM with chemical control	23.5	(Espiari et al., 2006)
20 to 76 °C, pH 2 to 3.5	SCM — diffusion control (hemi-morphite); SCM — chemical control (willemite)	49.2 (natural) 39.0 (synthetic) willemites	(Terry and Monhemius, 1983)
Smithsonite (9.6% Zn, 5.3% CaO, 15.1% SiO_2), column leaching, $(NH_4)_2SO_4$–NH_3	SCM — ash layer control	not determined	(Feng et al., 2007)
Electric arc furnace dust (ZnO, $ZnO{\cdot}Fe_2O_3$ and Fe_2O_3 (13.6% Zn, 29.8% Fe)). NaOH leach, 2% solids	Initial rate method	45.1	(Jarupisitthorn et al., 2003)
Willemite, franklinite (43.5% Zn, 23.3% SiO_2), 0.2–1.0 mol/L H_2SO_4; 30–60 °C, 1% solids, 2.5 m^2/g	Grain pore model (GPM) — pore diffusion control	50.7	(Souza et al., 2007)
Willemite, franklinite (35.6% Zn, 11.7% Fe, 23.8% SiO_2), 0.2–1.0 mol/L H_2SO_4; 10–50 °C, 1% solids, 0.6 m^2/g	GPM — pore diffusion control	78.2	(Souza et al., 2009)
Willemite, franklinite (46.9% Zn, 3.2% Fe, 29.6% SiO_2), 0.2–1.0 mol/L H_2SO_4; 30–70 °C, 1% solids, 0.5 m^2/g	GPM — pore diffusion control	67.0	(Souza et al., 2009)

layer control for the ammonia leaching of a pelletized zinc ore but did not determine the activation energy or the reaction order.

The present work shows that the kinetics of sodium hydroxide leaching of zinc silicate is chemically controlled with an activation energy of 67.8 ± 9.0 kJ/mol.

4. Conclusions

The alkaline leaching kinetics of a zinc silicate ore assaying 34.1% Zn, 11.1% Fe and 22.9% SiO_2 was studied. Speciation diagram indicates zinc dissolution as $[Zn(OH)_4]^{2-}$ and SEM analysis showed a progressive reduction in particle size during leaching which supported the application of the shrinking particle model to the leaching data. The process appears to be chemically controlled with an activation energy of as 67.8 ± 9.0 kJ/mol and a reaction order with respect to NaOH of 1.44 ± 0.46.

Notation

$[i]$	Molar concentration of species i
A	Surface area
k	Chemical rate constant
k_0	Arrhenius pre exponential factor
K_{app}	Apparent chemical reaction rate constant for non porous particles
n	Reaction order
R_0	Initial particle radius
t	Time
E_a	Activation energy
R	Universal gas constant ($8.314\,J\,mol^{-1}\,K^{-1}$)
T	Temperature
α	Conversion
ρ_{solid}	Silicate molar density

Acknowledgements

The financial support for this work from CNPq, FINEP and FAPEMIG is gratefully appreciated. The CAPES and CNPq scholarships to P. S. Pina, V. A. Leão, F. M. F Santos and R. Porcaro are also acknowledged.

References

Abdel-Aal, E.A., 2000. Kinetics of sulfuric acid leaching of low-grade zinc silicate ore. Hydrometallurgy 55 (3), 247–254.
Apostolidis, C.I., Distin, P.A., 1978. The kinetics of the sulphuric acid leaching of nickel and magnesium from reduction roasted serpentine. Hydrometallurgy 3 (2), 181–196.
Boateng, D.A.D., Phillips, C.R., 1984. Interpretation of the leaching kinetics of pentlandite in a complex system by the shrinking core model. Industrial and Engineering Chemistry Process Design and Development 23 (3), 557–561.
Bobeck, G., Su, H., 1985. The kinetics of dissolution of sphalerite in ferric chloride solution. Metallurgical and Materials Transactions B 16 (3), 413–424.
Bodas, M.G., 1996. Hydrometallurgical treatment of zinc silicate ore from Thailand. Hydrometallurgy 40 (1–2), 37–49.
Chen, A., et al., 2009. Alkaline leaching Zn and its concomitant metals from refractory hemimorphite zinc oxide ore. Hydrometallurgy 97 (3–4), 228–232.
Dutra, A.J.B., Paiva, P.R.P., Tavares, L.M., 2006. Alkaline leaching of zinc from electric arc furnace steel dust. Minerals Engineering 19 (5), 478–485.
Espiari, S., Rashchi, F., Sadrnezhad, S.K., 2006. Hydrometallurgical treatment of tailings with high zinc content. Hydrometallurgy 82 (1–2), 54–62.
Feng, L., Yang, X., Shen, Q., Xu, M., Jin, B., 2007. Pelletizing and alkaline leaching of powdery low grade zinc oxide ores. Hydrometallurgy 89 (3–4), 305–310.
Frenay, J., 1985. Leaching of oxidized zinc ores in various media. Hydrometallurgy 15 (2), 243–253.
Georgiou, D., Papangelakis, V.G., 1998. Sulphuric acid pressure leaching of a limonitic laterite: chemistry and kinetics. Hydrometallurgy 49 (1–2), 23–46.
Ghosh, M.K., Das, R.P., Biswas, A.K., 2002. Oxidative ammonia leaching of sphalerite. Part I: noncatalytic kinetics. International Journal of Mineral Processing 66, 241–254.
Habashi, F., 1993. A Textbook of Hydrometallurgy. Métallurgie Extractive Quebec, Quebec, 689 p.
Hursit, M., Laçin, O., Saraç, H., 2009. Dissolution kinetics of smithsonite ore as an alternative zinc source with an organic leach reagent. Journal of the Taiwan Institute of Chemical Engineers 40 (1), 6–12.
Jarupisitthorn, C., Pimtong, T., Lothongkum, G., 2003. Investigation of kinetics of zinc leaching from electric arc furnace dust by sodium hydroxide. Materials Chemistry and Physics 77 (2), 531–535.
Levenspiel, O., 1962. Chemical Reaction Engineering. John Wiley & Sons, New York. 578 pp.
Martell, A.E., Smith, R.M., 2003. NIST Critically Selected Stability Constants of Metals Complexes. National Institute of Standards and Technology, Gaithersburg, MD.
Massaci, P., Recinella, M., Piga, L., 1998. Factorial experiments for selective leaching of zinc sulphide in ferric sulphate media. International Journal of Mineral Processing 53, 213–224.
Safari, V., Arzpeyma, G., Rashchi, F., Mostoufi, N., 2009. A shrinking particle–shrinking core model for leaching of a zinc ore containing silica. International Journal of Mineral Processing 93 (1), 79–83.
Senanayake, G., 2007. Review of rate constants for thiosulphate leaching of gold from ores, concentrates and flat surfaces: effect of host minerals and pH. Minerals Engineering 20 (1), 1–15.
Souza, A.D., 2007. Cinética de lixiviação dos concentrados de zinco utilizados na Votorantim Metais. PhD. Thesis, Universidade Federal de Ouro Preto, Ouro Preto, MG,Brazil, 112 pp. http://www.redemat.ufop.br/arquivos/teses/2007/cinetica%20de%20lixiviacao.pdf.
Souza, A.D., Pina, P.S., Lima, E.V.O., Silva, C.A., Leao, V.A., 2007. A kinetic study of the sulphuric acid leaching of a zinc silicate calcine. Hydrometallurgy 89, 337–345.
Souza, A.D., Pina, P.S., Santos, F.M.F., da Silva, C.A., Leão, V.A., 2009. Effect of iron in zinc silicate concentrate on leaching with sulphuric acid. Hydrometallurgy 95 (3–4), 207–214.
Szekely, J., Evans, J.W., Sohn, H.Y., 1976. Gas Solid Reactions. Academic Press, New York. 400 pp.
Teir, S., Revitzer, H., Eloneva, S., Fogelholm, C.-J., Zevenhoven, R., 2007. Dissolution of natural serpentinite in mineral and organic acids. International Journal of Mineral Processing 83 (1–2), 36–46.
Terry, B., Monhemius, A.J., 1983. Acid dissolution of willemite ((Zn, Mn)2SiO4) and hemimorphite (Zn4Si2O7(OH)2H2O). Metallurgical Transactions B—Process Metallurgy 14 (3), 335–346.
Xia, D.K., Picklesi, C.A., 2000. Microwave caustic leaching of electric arc furnace dust. Minerals Engineering 13 (1), 79–94.
Zaky, R.R., et al., 2008. Preparation of silica nanoparticles from semi-burned rice straw ash. Powder Technology 185 (1), 31–35.
Zhao, Y., Stanforth, R., 2000. Production of Zn powder by alkaline treatment of smithsonite Zn–Pb ores. Hydrometallurgy 56 (2), 237–249.